Available online at www.sciencedirect.com
ScienceDirect
Geochimica et Cosmochimica Acta 71 (2007) 2056–2071
Geochimica et Cosmochimica Acta
www.elsevier.com/locate/gca

Trace element partitioning between vapor, brine and halite under extreme phase separation conditions

D.I. Foustoukos *, W.E. Seyfried Jr.

Department of Geology and Geophysics, University of Minnesota, Minneapolis, MN 55455, USA

Received 20 September 2006; accepted in revised form 31 January 2007; available online 2 February 2007

Abstract

Experiments were conducted to investigate the partitioning of Li, Br, Rb, Cs and B between vapor, brine and halite during subcritical and supercritical phase separation in the NaCl–H_2O system (388–550 °C, 250–350 bars). Results indicate that Li and Br partition preferentially into the low-salinity vapor fluids, while Rb and Cs become more enriched in the coexisting brines. Under more extreme conditions of pressure and temperature in the two-phase region, especially near the vapor–brine–halite boundary, strong *salting-out* effects imposed on neutral aqueous species enhance significantly partitioning of all trace elements into the low-salinity fluid. Dissolved boron is strongly affected by this and a particularly strong enrichment into vapors is observed, a trend that can be effectively correlated with changes in reduced density. Exclusion of Li, Br, Rb, Cs and B from halite, when precipitated, further increases the solubility of these species in the coexisting Cl-poor fluid. In general, the lack of distortion in the partitioning behavior of trace elements between vapor, brine and/or halite with the transition from subcritical to supercritical conditions in the NaCl–H_2O system precludes the need for special reference to the critical point of seawater when interpreting phase relations in submarine hydrothermal systems. The combination of experimentally determined trace element partitioning data with constraints imposed by mineral solubility provides a means to better understand the origin and evolution of hot spring vent fluids. For example, in Brandon hydrothermal system (21°S EPR) supercritical phase separation and subseafloor mixing appear to be the main heat and mass transport mechanisms fueled by a shallow magmatic intrusion, with boron systematics ruling out major contributions from magmatic degassing processes accompanying the near-seafloor volcanism.

1. INTRODUCTION

Phase separation in the NaCl–H_2O system is now commonly recognized as one of the dominant processes affecting heat and mass transport in mid-ocean ridge hydrothermal systems (Bischoff and Rosenbauer, 1987; Butterfield et al., 1994; Von Damm et al., 1995; Berndt and Seyfried, 1997; Von Damm, 2000; Seyfried et al., 2003). This is indicated best by the deviation from seawater values of the dissolved chloride concentrations in vent fluids issuing from mid-ocean ridge hot springs (Oosting and Von Damm, 1996; Berndt and Seyfried, 1997; Von Damm et al., 1997; Fornari et al., 1998; Butterfield et al., 1999; Von Damm, 2000; Lilley et al., 2003; Seyfried et al., 2003).

Phase separation of Cl-bearing aqueous fluids can occur at a wide range of temperature and pressure conditions (Fournier, 1986; Bischoff, 1991), resulting in the formation of conjugate pairs of low (“vapors”) and high (“brines”) salinity/density aqueous solutions that can be quantitatively described by now well-established phase relations in the NaCl–H_2O system (Bischoff and Rosenbauer, 1984; Bischoff and Rosenbauer, 1988; Bischoff, 1991; Berndt et al., 2001). Under extreme phase separation conditions (P, T, x), the halite field of stability may be encountered, which acts as an additional constraint on the composition of coexisting Cl-bearing phase(s) (Berndt and Seyfried, 1997). Phase separation-induced changes in dissolved Cl

* Corresponding author. Present address: Geophysical Laboratory, Carnegie Institution of Washington, 5251 Broad Branch Road, NW, Washington, DC 20015, USA. Fax: +1 202 478 8901.
E-mail address: dfoustoukos@ciw.edu (D.I. Foustoukos).

0016-7037/$ - see front matter © 2007 Elsevier Ltd. All rights reserved.
doi:10.1016/j.gca.2007.01.024

can affect bulk fluid composition owing to homogeneous and heterogeneous equilibria effects (Von Damm, 2000; Seyfried et al., 2003). For example, the Br/Cl ratios of vent fluids at 9–10°N East Pacific Rise (EPR) have been interpreted to indicate halite precipitation/dissolution processes directly linked to phase separation phenomena, which cause these ratios to significantly deviate from seawater values (Oosting and Von Damm, 1996; Berndt and Seyfried, 1997).

The highly incompatible trace alkali elements (Li, Rb, Cs) and B have long been considered important indicators of subseafloor chemical and physical processes (Spivack and Edmond, 1987; Palmer and Edmond, 1989; Chan et al., 1993; Seyfried et al., 1998). Indeed, temporal variability of dissolved Li and B concentrations in Cl-depleted fluids issuing from vents at the Main Endeavour Field on the Juan De Fuca Ridge (MEF-JDF), suggest that these elements may be useful tracers of subseafloor magmatic activity and phase separation processes (Foustoukos et al., 2004). Quantitative constraints on subseafloor hydrothermal processes are possible when sufficient experimental data are available to establish the role of temperature, pressure and dissolved chloride on the distribution of these species between coexisting phases. Insights from field data from subaerial magmatic/hydrothermal systems have underscored the potential usefulness of the partitioning of theses elements between vapors and brines to constrain subsurface geochemical processes (Audetat et al., 1998).

Previous experimental studies conducted to investigate the distribution of Li, Br and B in supercritical/subcritical vapors and brines (Bischoff and Rosenbauer, 1987; Berndt and Seyfried, 1990; Berndt and Seyfried, 1997; Liebscher et al., 2005) were restricted in temperature and pressure, as well as limited by the close-system experimental approaches adopted. The relatively high contrast in density and composition between coexisting vapors and brines anticipated for physical conditions deep in the two-phase region (Bischoff, 1991; Berndt et al., 2001), presents serious experimental challenges for a closed and fixed volume gold reaction cell (Seyfried et al., 1987). Thus, existing experimental data describe elemental partitioning at pressures and temperatures in the close vicinity of the NaCl–H_2O critical curve (Fig. 1). In order to investigate trace element partitioning under more realistic conditions of phase separation, an open-system experimental approach is necessary, one that provides sufficient volume to accommodate low-density vapor phases.

Here, we present experimental data for the partitioning of trace elements between vapor and brine obtained during hydrothermal experiments performed in a flow-through reactor at a wide range of pressures and temperatures (Fig. 1). In details, experiments involved formation of conjugate vapor/brine pairs along the 250, 300, and 350 isobars and at temperatures ranging from 388 to 550 °C, stimulating subcritical and supercritical phase separation processes (critical point of seawater: 410 °C—300 bars). Most importantly, experimental data from the halite–vapor system were obtained, allowing for first time the halite stability field to be reached, while monitoring the composition of coexisting low-density vapors.

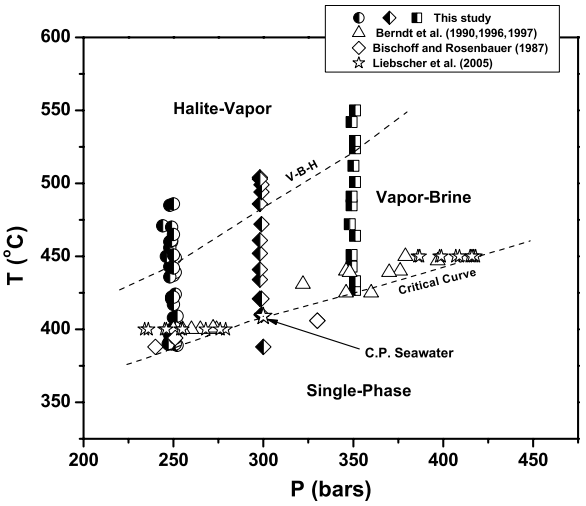

Fig. 1. Diagram depicting the range of pressure and temperature conditions investigated during trace element partitioning experiments in the NaCl–H_2O system. Sub- and supercritical phase separation phenomena were established along 250, 300 and 350 isobars, while temperatures ranged from 388 to 550 °C. In contrast, previous experimental studies were conducted at pressures and temperatures close to the NaCl–H_2O critical curve, limiting in this way our understanding in trace element partitioning between vapor, brine and halite phases. Phase relationships in the NaCl–H_2O system are described by Berndt et al. (2001).

Experimentally derived partition coefficients for Br and B are especially needed for constraining phase separation and water/rock interaction processes in subseafloor reaction zone of the vent fields near 21°S on EPR where chemical and physical data suggest existence of unusually high temperatures and pressures. Fluids issuing from vents at this site exhibit some of the highest temperatures ever measured (~404 °C) with dissolved chloride concentrations (~300 mmol/kg_{sol}), suggesting near-seafloor phase separation phenomena linked to a shallow heat source (Von Damm et al., 2003). The trace alkali and B data may allow the near-seafloor model of phase separation to be quantitatively examined.

The experimental data for these and other species also permit a more general examination of the transition from subcritical to supercritical phase separation on the direction and magnitude of partitioning between vapors and brines. Thus, data can provide a better understanding of whether partitioning behavior changes abruptly from one critical condition to the other or is a continuous process, governed more by fundamental characteristics of the aqueous system at a given temperature, pressure and bulk composition.

2. METHODS

2.1. Experimental procedures and design

Experiments, reported here, were conducted using a novel experimental approach involving a flow-through hydrothermal reactor to simulate open-system conditions. In effect, the experimental system included a fixed volume

(103 ml) flow cell (Fig. 2), which was connected to a series of high-pressure metering pumps (Shimatsu LC-10A, Bischoff HPLC 2250), facilitating continuous flow of source fluid at constant pressure and flow rate. To more accurately regulate pressure, however, the outlet side of the reactor was connected to a computer-controlled metering valve. Accordingly, the rate of fluid input and output as well as the total pressure of the system were precisely and accurately maintained at pre-selected values throughout the experiment.

Phase separation experiments are extremely pressure and temperature sensitive, since slight changes in conditions can cause significant changes in the chemical composition of coexisting vapor/brine pairs in the two-phase region of the NaCl–H_2O system (Bischoff, 1991; Berndt et al., 2001). Thus, an essential part of the experimental configuration is the need for accurate monitoring of pressure and temperature of the fluid throughout the flow cell. To meet this need, *J*-type thermocouples (Fe-constantan) were placed directly within the vessel and in contact with the aqueous solutions (Fig. 2). Watlow time proportioning controllers with auto tuning capabilities regulated power to a series of band heaters external to the reactor, each of which could be independently controlled. Simultaneous monitoring of pressure was established by a Heise ST-2H digital pressure indicator, which served as an additional check on pressure provided by the fluid delivery system described above. The high precision pressure transducer is accompanied with a NIST traceable certificate of calibration (www.heise.com), limiting pressure uncertainties to 0.025% of the operating pressure. Temperature uncertainties are ±1 °C based on previous calibrations conducted with steam-saturated water at 300–360 °C (Foustoukos and Seyfried, 2007). Both temperature and pressure measurements were digitally recorded through RS-232 communications, allowing P–T conditions to be continuously monitored during the length of fluid flow and sampling procedure.

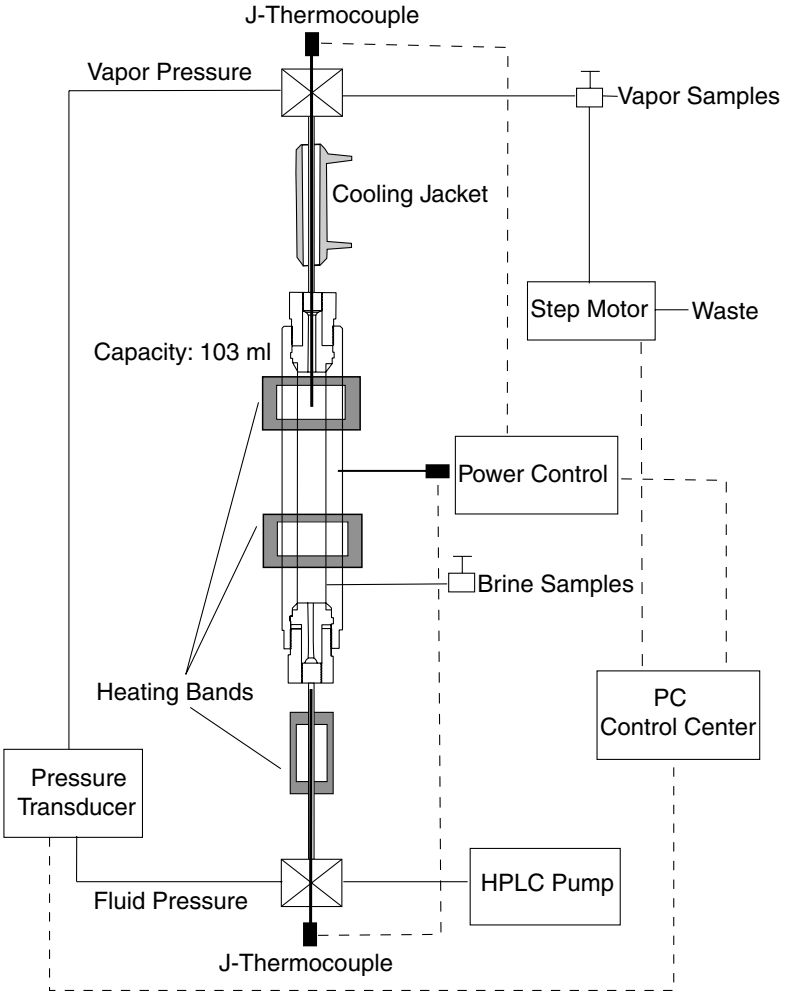

Fig. 2. Schematic illustration of the flow-through reaction cell utilized to study trace element fractionation during phase separation in the NaCl–H_2O system. The use of an open-system approach allows supercritical and low-density vapors to be formed at temperatures up to 550 °C. Constant flow and pressure conditions were maintained by an array of pressure regulators including in-line pressure transducer, HPLC pump and a stepper motor. Thermocouples, placed at the both ends of the reactor, monitored temperature of the escaping vapors (top) and that of the pre-heated homogeneous reactant fluid (bottom).

The phase separation experiments were performed at conditions representing the vapor–brine and halite–vapor region of the NaCl–H_2O system (Fig. 1). Thus, the starting fluid was a 3.2 wt% NaCl aqueous solution enriched with trace amounts of Br, Li, Rb, Cs and B. Phase separation was induced by incremental increase of temperature, while maintaining constant pressure conditions in the flow cell. To more effectively induce phase separation, however, the source fluid was preheated to 370 °C prior to entering the reaction chamber (Fig. 2). Moreover, to better permit segregation of the buoyant vapor from the more dense brine, the hydrothermal reactor was positioned in an upright orientation, which facilitated retrieval of pure vapors and brine samples.

Fluids were analyzed for Li, Br, Rb, Cs and B by ICP-MS, while Cl and Na were measured by ion-chromatography (IC). Uncertainties in reported concentrations of the major dissolved elements (e.g. Na, Cl) are estimated to be $\pm 2\%$ at the 1σ level, whereas for the trace elements the uncertainty is approximately $\pm 5\%$ indicated by replicate measurements and comparison tests using both IC and ICP-MS techniques. Fluid composition is described in $mol/kg_{solution}$ units to be consistent with concentration expressions used in the oceanographic community.

2.2. Theoretical modeling

Recent advances in the dissociation equilibria of 1:1 aqueous complexes ($NaCl_{(aq)}$, $LiCl_{(aq)}$, $HCl_{(aq)}$, $NaOH_{(aq)}$, $LiOH_{(aq)}$) at low water-density conditions (~ 0.3 g/cm^3) (Ho et al., 1994, 2000a,b, 2001), permit calculations of aqueous species distribution in the low-chloride fluids within the vapor–brine and vapor–halite stability fields. Aqueous speciation, however, is not yet plausible for the more saline brines due to the possible existence of polyatomic ionic species (Pitzer and Schreiber, 1987; Oelkers and Helgeson, 1990; Oelkers and Helgeson, 1993a,b; Driesner et al., 1998; Sharygin et al., 2002). Thermodynamic data for the Rb, Cs and Br aqueous species (Rb^+, Cs^+, Br^-, $RbCl_{(aq)}$, $RbBr_{(aq)}$, $RbOH_{(aq)}$, $CsCl_{(aq)}$, $CsOH_{(aq)}$, $CsBr_{(aq)}$, $NaBr_{(aq)}$) were retrieved from Sverjensky et al. (1997) and Shock et al. (1997), whereas for the B aqueous species ($B(OH)_4^-$, $B(OH)_{3(aq)}$, $NaB(OH)_{4(aq)}$) data were derived from Pokrovski et al. (1995). Activity coefficients for charged aqueous species were calculated using the extended Davies model (Davies, 1962) following methodologies described in Foustoukos and Seyfried (2007).

Results from the preliminary speciation modeling support significant formation of neutral complexes ($B(OH)_{3(aq)}$, $NaBr_{(aq)}$, $NaCl_{(aq)}$, $LiCl_{(aq)}$, $RbCl_{(aq)}$, $CsCl_{(aq)}$) under low water-density conditions, as it has previously been suggested by theoretical studies that take into account the effect of weakened dielectric constant of H_2O on the distribution of neutral-charged aqueous complexes (Oelkers and Helgeson, 1990; Sharygin et al., 2002; Sue and Arai, 2004). Considering the abundance of chloro-complexes and the dominance of $NaCl_{(aq)}$ in the reactant fluids, Br, Li, Rb and Cs partitioning coefficients between vapor and brine/halite phases can be expressed as elemental ratios with Cl

$$D_{el/Cl} = \frac{(M_{el}/M_{Cl})_v}{(M_{el}/M_{Cl})_b} \quad (1)$$

where $(M_{el}/M_{Cl})_v$ and $(M_{el}/M_{Cl})_b$ are the elemental chloride ratios for vapors and brines/halite, respectively. $D_{el/Cl}$ values greater than unity indicate the preferential fractionation into the vapor phase, while the opposite (brine enrichment) is true when $D_{el/Cl}$ is less than 1.

Elemental fractionation can also be expressed as apparent vapor–brine partitioning coefficients K_m

$$K_m = (M_{el})_v/(M_{el})_b \quad (2)$$

where $(M_{el})_v$ and $(M_{el})_b$ designates the total dissolved concentrations of each element in the corresponding phase. K_m values, when correlated with the density of vapor and brine fractions, have been shown to model accurately the relative tendency for vapor partitioning and the overall hydration of the dissolved elements in chloride-bearing fluids (Palmer et al., 2004; Pokrovski et al., 2005).

Comparisons between predicted and measured chloride concentrations of vapors and coexisting brines can provide additional confidence in the overall interpretation of the experimental data depicting phase relationships in the NaCl–H_2O system. In general, the bulk composition and density of the vapor/brine endmembers can be assessed by vapor–brine equilibrium tables as summarized in Bischoff (1991). Advances in thermodynamic modeling, however, allow a more detailed analysis of these data. Indeed, by making use of the mathematical model *Salt-Therm 1.0* (Berndt et al., 2001), accurate estimations of the dissolved Cl concentrations in vapor–brine conjugated pairs over a wide range of conditions are possible. The code includes an integrated compilation of compositional and density data retrieved from NaCl–H_2O experiments and theoretical studies (Haas, 1976a,b; Pitzer et al., 1984; Tanger and Pitzer, 1989; Bischoff, 1991; Anderko and Pitzer, 1993). More specifically, density, viscosity, temperature and the corresponding phase relations are stored as multispline functions of enthalpy, pressure and salinity. Expressing these physical properties as enthalpy-based functions provides smoothly fitted and detailed estimations of the NaCl–H_2O phase relationships along a wide range of pressure and temperature conditions (Mercer and Faust, 1979; Hayba and Ingebritsen, 1994). Previous studies have successfully implemented the code to investigate the chemical and thermal evolution of the low-salinity vent fluids at the MEF-JDF, providing evidence of supercritical conditions controlling water/rock interactions deep in the roots of the hydrothermal system (Seyfried et al., 2003). A less intricate approach is followed for the pure H_2O system, with thermodynamic properties calculated from Sengers et al. (1983) and Haar et al. (1984) equations of state.

Statistical analysis of the experimental data was conducted using the package *Arc 1.06* (http://www.stat.umn.edu/arc) (Cook and Weisberg, 1999). The software is structured based on Lisp-Stat (Tierney, 1989), permitting data analysis by utilizing dynamic graphical methods.

3. RESULTS

A series of 5 experiments was performed to assess trace element vapor–brine–halite fractionation patterns under subcritical (250 bars) and supercritical (300–350 bars) conditions in the NaCl–H_2O system (Fig. 1). The majority of samples analyzed, however, were low-salinity vapor phases produced in the vapor–brine and halite–vapor stability fields (Table 1). The scarcity of pure brine samples (experiment 1—sample 1, experiment 2—sample 3), reflects the difficulties of withdrawing the small amount of brine generated for the chemical and physical conditions, especially in the vicinity of the halite stability (Bischoff, 1991). For the vapor and brine samples that were obtained, pressure and temperature conditions remained constant during acquisition (Table 1) by system controls, precluding compositional modification during the sampling process. Dissolved Cl concentrations of the samples are in excellent agreement with concentrations predicted from phase relations in the NaCl–H_2O system (Berndt et al., 2001) (Fig. 3). Results indicate that vapor–brine equilibrium was attained, and no entrainment of high-salinity fluids occurred during sampling of the vapor fractions.

Confidence developed on the high quality of vapor phases collected, allowed the chemical composition of the conjugate brines to be determined following simple mass balance constraints as described by Berndt et al. (1996):

$$X_{\text{brine}}\text{Salinity}_{\text{brine}} + X_{\text{vapor}}\text{Salinity}_{\text{vapor}} = \text{Salinity}_{\text{bulk}} \quad (3)$$

$$X_{\text{brine}} + X_{\text{vapor}} = 1 \quad (4)$$

$$X_{\text{brine}}M_{\text{brine}} + X_{\text{vapor}}M_{\text{vapor}} = M_{\text{bulk}} \quad (5)$$

where X_{brine} and X_{vapor} stand for the mass fractions of brine and vapor, respectively, while M_{brine} and M_{vapor} designates the total dissolved concentrations of each element of the subscripted phases.

Owing to charge balance constraints, and aqueous speciation effects, it is not surprising that the absolute concentrations of trace element species (Na, Li, Cs, Rb) follow dissolved chloride with increasing phase separation in the NaCl–H_2O system. This was also the case for Br because of the apparent stability of $NaBr_{(aq)}$ (Table 1). At relatively high temperatures and low to moderate pressures, especially near the vapor–brine–halite boundary (Fig. 1), trace element concentrations *on a chloride-normalized basis* increase in the vapor fraction, although this is significantly greater for Br/Cl and Li/Cl than for Rb/Cl and Cs/Cl (Fig. 4a). This behavior is most likely caused by *salting-out* effects imposed on neutral aqueous species dissolved in the increasingly concentrated brine (Pitzer and Schreiber, 1987; Oelkers and Helgeson, 1990; Oelkers and Helgeson, 1993a,b; Sharygin et al., 2002; Grover and Ryall, 2004). This becomes even more noticeable with halite precipitation (Fig. 4a), which may relate to the additional effect of the strongly immiscible nature of trace elements in the halite structure. This is especially well recognized for Br (Stoessel and Carpenter, 1986; Stoessel, 1992; Berndt and Seyfried, 1997) but may affect the other species as well. The overall lagging trends revealed by Rb/Cl and Cs/Cl, however, may be caused by constraints introduced by differences in cation–anion electronegativity for the $CsCl_{(aq)}$, $RbCl_{(aq)}$, $LiCl_{(aq)}$ and $NaBr_{(aq)}$ aqueous species (Berndt and Seyfried, 1990) (Fig. 4a). *Salting-out* effects also influence $HCl_{(aq)}$, accounting in part for the pH[1] decrease observed in vapors (Table 1; Fig. 4b), which agrees well with results of previous experimental and theoretical studies (Bischoff et al., 1996; Pokrovski et al., 2002; Heinrich et al., 2004; Sue and Arai, 2004).

As pressures and temperatures representing conditions deep in the two-phase region are investigated, increases in boron concentrations in vapors are observed. This can be attributed to a number of factors including *salting-out* effects, as well as to the polar gas-like behavior of boron, which under low pH conditions renders the neutral $B(OH)_{3(aq)}$ species stable (Styrikovich et al., 1960; Berndt and Seyfried, 1990; Schmidt et al., 2005). Again, following patterns observed for halide-bonded alkaline and alkaline earth elements, dissolved boron concentrations in the vapor are enhanced subsequent to halite precipitation (Table 1). On a chloride-normalized basis (Fig. 4b), however, a surprisingly linear correlation is observed, which exists over a wide range of chemical and physical conditions. This strongly supports a conservative behavior of boron during extreme phase separation; an observation that has important implications for distinguishing fluid/rock interaction and phase separation effects on boron in submarine and epithermal hydrothermal systems.

4. DISCUSSION

To better understand trace element partitioning between vapor, brine and halite, quantitative analysis of the apparent (K_m) and the Cl-normalized ($D_{el/Cl}$) partitioning coefficients is required. Fractionation patterns, however, can be also expressed in terms of the salinity contract between Cl-bearing phases and H_2O density. As can be inferred from above, elevated dissolved salt concentrations enhance *salting-out* effects, which enrich neutral aqueous species in the low-salinity vapor. Changes in the density of water, however, influence the thermodynamic properties of dissolved species on a more fundamental level, and thus, can be used to constrain the partitioning of species between vapor and brines over a broad range of pressure–temperature conditions.

4.1. Apparent partitioning coefficients

One formulation to express vapor–brine distribution is to describe apparent partitioning coefficients as a function of the density contrast between coexisting phases. This approach has been widely used for studies involving mass transport in steam (Styrikovich et al., 1955; Smith et al., 1987; Simonson et al., 2000; Pokrovski et al., 2002; Palmer et al., 2004) and for Cl-enriched vapors produced during supercritical phase separation (Pokrovski et al., 2005). Representation of the relationship between K_m and the densities

[1] pH measured at 25 °C—1 bar.

Table 1
Chemical composition of fluid samples collected during phase separation experiments in the multiphase NaCl–H_2O system

Phase region[a]		T (°C)	P (bars)	Cl (mM)[b]	Na (mM)	B (μM)	Li (μM)	Br (μM)	Rb (μM)	Cs (μM)	Salinity wt% NaCl	pH[c]
Experiment 1												
	Start			576	566	5023	557	1377	174	97	3.365	6.9
v–**b**	1	390	249	1158	1155	11147	1442	2910	364	202	6.770	6.8
v–b	2	392 ± 1	250 ± 1	76	76	3086	99	201	22	12	0.445	6.2
v–b	3	392 ± 1	248	42	42	3335	57	118	12	6.7	0.244	5.3
v–b	4	400 ± 2	249	21	21	3940	32	61	5.4	2.8	0.121	3.9
v–b	5	408 ± 1	250	25	25	3660	39	73	7.7	4.2	0.148	5.4
v–b	6	421 ± 1	249	13	10	4527	20	42	2.3	1.3	0.075	4.9
v–b–h	7	443 ± 1	248 ± 1	5	5	4619	73	64	15	8.2	0.030	4.4
v–h	8	450 ± 1	246	4	4	4992	27	46	6.3	3.5	0.025	4.2
v–h	9	460 ± 1	249	3	3	4905	21	48	3.7	2.1	0.020	4.2
v–h	10	471	244	3	3	5504	108	102	48	28	0.018	4.4
Experiment 2												
	Start			583	575	4743	573	1359	173	682	3.410	6.5
v–b	1	389	252 ± 1	114		3520	94	285	34	132	0.665	5.6
v–b	2	390	251 ± 1	32		3611	29	103	10	40	0.189	5.4
v–**b**	3	390 ± 1	247	1197	1180	6014	1000	2851	369	1451	6.996	6.2
v–b	4	400 ± 1	252	15	14	4073	13	43	3.3	12	0.085	5.2
v–b	5	396 ± 1	248 ± 1	13	12	3971	12	45	2.7	10	0.074	5.0
v–b	6	409 ± 1	252	11	11	3785	12	36	2.2	8.2	0.065	5.0
v–b	7	422 ± 1	249 ± 1	8	7	4305	13	30	1.4	5.1	0.044	4.5
v–b	8	424 ± 1	251	8	7	4488		34	1.6	5.7	0.044	4.6
v–b	9	437 ± 1	250	5	4	4890	27	82	7.7	31	0.028	4.1
v–b	10	439 ± 1	251	5	4	4459	36	73	9.1	37	0.028	4.0
v–b	11	436 ± 1	248 ± 1	5	5	4636	26	42	4.2	17	0.032	4.0
v–b–h	12	456 ± 1	248	4	4	4940	20	45	8.1	33	0.023	3.8
v–h	13	460 ± 1	248	3	3	5494	22	60	8.2	33	0.020	3.8
v–h	14	470 ± 1	249	3	3	6264	32	102	18	74	0.018	3.6
v–h	15	485 ± 1	248	3	2	6404	39	134	29	126	0.017	3.5
v–h	16	486 ± 3	250 ± 2	3	2	6651	86	173	41	193	0.015	3.5
Experiment 3												
	Start			574	556	11563	733	593			3.357	
v–b	1	394 ± 1	251 ± 1	48	49	7185	70	56			0.283	
v–b	2	401 ±1	251	20	20	7691	30	29			0.116	
v–b	3	417 ± 1	250 ± 1	10	10	9463	16	24			0.058	
v–b–h	4	422 ± 3	250 ± 1	7	7	10777	15	17			0.040	
v–h	5	449 ± 1	251 ± 1	4	4	11656	133	47			0.023	
v–h	6	442 ± 1	250	6	5	9343	84	24			0.033	
v–h	7	451 ± 1	250	5	5	11628	36	26			0.029	
v–h	8	461 ± 3	249 ± 1	4	3	13182	37	28			0.022	
v–h	9	465 ± 2	250 ± 1	4	3	13330	98	52			0.021	
Experiment 4												
	Start			573	617	4601	667	1461	188	99	3.351	
	1	388 ± 1	300	570	594	3981	644	1463	190	99	3.331	
v–b	2	410 ± 1	299	308	308		306	660	77	40	1.800	
v–b	3	421 ± 1	298 ± 1	53	57	4196	72	154	14	7.2	0.310	
v–b	4	421 ± 1	299 ± 1	35	37	3774	52	107	8.5	4.3	0.207	
v–b	5	434 ± 1	298 ± 1	24	27	4413	40	77	5.2	2.7	0.142	
v–b	6	441 ± 1	298 ± 1	21	22	4552	37	75	4.5	2.4	0.123	
v–b	7	452 ± 1	298 ± 1	16	18	5119	33	60	3.1	1.7	0.093	
v–b	8	461	298 ± 1	13	16	5569	32	60	2.8	1.4	0.077	
v–b	9	472 ± 1	299 ± 1	11	13	5393	27	53	2.5	1.2	0.064	
v–b–h	10	486 ± 1	298 ± 1	9	10	5205	33	70	6.7	3.7	0.051	
v–h	11	494 ± 2	299 ± 2	8	9	5430	28	54	3.6	2.0	0.047	
v–h	12	499 ± 1	299 ± 1	7	7	5242	30	54	5.2	2.9	0.039	
v–h	13	504	298 ± 2	6	8	6132	32	58	5.0	2.8	0.037	
v–h	14	503 ± 1	298 ± 1	6	9	8312	62	114	16	9.4	0.035	

(*continued on next page*)

Table 1 (*continued*)

Phase region[a]		T (°C)	P (bars)	Cl (mM)[b]	Na (mM)	B (μM)	Li (μM)	Br (μM)	Rb (μM)	Cs (μM)	Salinity wt% NaCl	pH[c]
Experiment 5												
	Start			563	575	4533	661	1249	180	70	3.291	6.5
v–b	1	427 ± 1	351 ± 1	518	522	3325	599	1135	165	64	3.026	6.4
v–b	2	433 ± 1	351	120	121	4159	155	294	33	12	0.704	5.6
v–b	3	443	349	55	56	4281	80	166	13	4.9	0.320	5.1
v–b	4	451 ± 1	349	39	40	4531	63	129	8.9	3.3	0.228	5.0
v–b	5	464 ± 1	351 ± 1	30	31	4343	52	101	6.7	2.6	0.177	4.8
v–b	6	472	348	25	26	4689	47	91	5.4	2.1	0.149	4.4
v–b	7	485 ± 1	349	20	20	4857	40	74	3.8	1.4	0.115	4.2
v–b	8	491 ± 1	349	17	18	5008	37	71	3.3	1.3	0.102	4.1
v–b	9	501 ± 1	351 ± 1	15	15	5172	33	65	2.7	1.1	0.085	4.0
v–b	10	512 ± 1	350 ± 1	13	13	4897	30	60	2.7	1.1	0.074	3.9
v–b–h	11	524 ± 1	351 ± 1	11	11	5355	33	59	3.9	1.5	0.063	3.9
v–h	12	529 ± 1	351 ± 1	11	11	5097	34	70	3.6	1.5	0.064	3.8
v–h	13	542 ± 1	349	10	10	5180	30	58	3.3	1.4	0.058	3.8
v–h	14	550 ± 1	351 ± 1	9	9	5367	36	84	8.2	3.4	0.051	3.8

[a] v–b, vapor–brine; v–b–h, vapor–brine–halite; v–h, vapor–halite. Sampled phases are shown in bold fonts.
[b] mM, mmol/$kg_{solution}$.
[c] pH at 25 °C—1 bar.

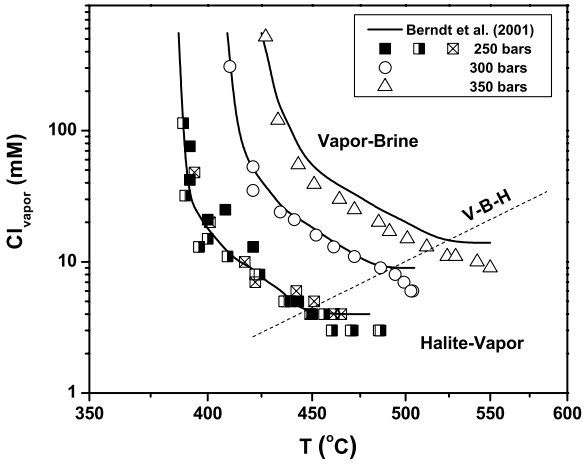

Fig. 3. Dissolved Cl concentrations of vapor samples collected during the present investigation. The excellent agreement between measured and predicted dissolved chloride concentrations demonstrates the effectiveness of the flow-through reactor to produce pure vapor endmembers that accurately reflect NaCl–H_2O phase relations (Berndt et al., 2001). Moreover, the high quality vapor fluids sampled further supports the lack of vapor–brine mixing and/or convection processes within the reaction cell, allowing reconstruction of the chemical composition of conjugate brine endmembers not directly collected.

of vapor–brine can be illustrated by means of a ray diagram constructed based on the following linear function:

$$\log K_m = n_i \log(\text{density}_{vapor}/\text{density}_{brine}) \quad (6)$$

where (n_i) is an empirical fitting coefficient linked to the vapor–brine hydration and the volatility of the aqueous species (Simonson et al., 2000; Palmer et al., 2004). Elevated positive values of (n_i) indicate less affinity of non-volatile components to fractionate into the vapor phase, while negative values characterize more volatile components (e.g. dissolved gases (Smith et al., 1987)) exhibiting negative hydration behavior. Recently, this approach has been successfully deployed to assess vapor–liquid partitioning of dissolved metals under low water-density conditions (Pokrovski et al., 2005).

A ray diagram based on apparent partitioning coefficients of trace elements in coexisting vapor–brine pairs confirms the tendency of species to partition into the low-salinity vapor (Fig. 5). For example, results indicate (n) value for Br of 2.99 (±0.03), consistent with the number of hydration waters ($N < 3$) expected for elemental hydration at supercritical H_2O conditions (424 °C) (Wallen et al., 1997), while Li with (n_{Li}) of 3.01 (±0.05) is in close agreement with data from previous experimental vapor–liquid fractionation studies ($n_{Li} \sim 3.25$) (Styrikovich, 1956; Smith et al., 1987). Values (n) of 3.44 (±0.05) and 3.46 (±0.05) were calculated for Rb and Cs, respectively, which are consistent with the low Rb hydration ($N = 3.9$) measured in XAFS studies under supercritical conditions (Fulton et al., 1996). Thus, the overall partitioning into vapors decreases in the order of Li ≅ Br > Rb ≅ Cs, indicating a general decrease in vapor-phase hydration and species volatility.

In the case of boron, however, the significantly lower (n_B) value of 0.52 (±0.1) (Fig. 5), indicates a strong volatile behavior and a clear enhanced affinity to participate in vapor enrichment consistent with other vapor–liquid partitioning experiments ($n_B = 0.9$) (Styrikovich et al., 1960). The scattering in the B data, however, suggests limitations in the ray diagrams when applied to solutes that form pH-dependent hydroxyl-bearing aqueous species (Palmer et al., 2004). Nevertheless, boron, most likely existing as $B(OH)_{3(aq)}$ (Table 1) (Pokrovski et al., 1995; Schmidt et al., 2005), appears to attain a similar range of (n_B) values as other volatile neutral hydroxide species, such as As $(OH)_{3(aq)}$ (Pokrovski et al., 2005), reinforcing the notion that boron partitioning in phase separated hydrothermal systems is largely controlled by the strong volatility of the

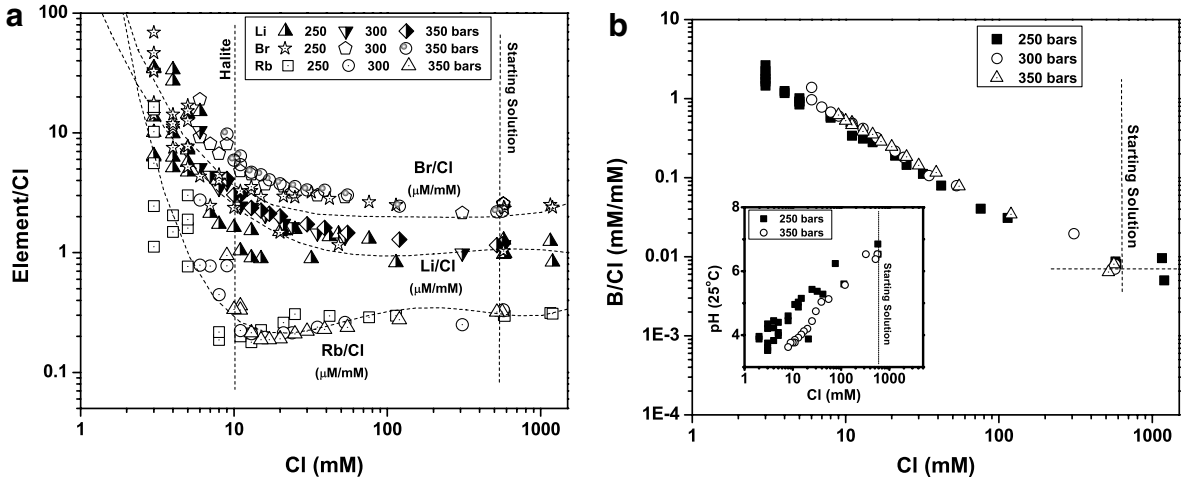

Fig. 4. Chloride-normalized concentrations of dissolved trace elements in vapor samples corresponding to vapor–brine and halite–vapor stability fields. (a) Results indicate an overall enrichment of Li and Br into vapor phases, while the opposite is true for Rb and Cs (not shown). These data are consistent with predictions based on electronegativity differences between cation–anions constituting the dominant neutral aqueous species. Precipitation of halite, however, favors enhanced partitioning of trace elements into the vapor phase, supporting the immiscible behavior of trace elements in highly ionic fluid/mineral phases. (b) In the case of boron, Cl-normalized data indicate a linear and steady enrichment in vapor phases, which appear to be indistinguishable for all the pressure–temperature conditions visited. This conservative behavior of B can be attributed to *salting-out* effects and the "volatility" of the dominant neutral aqueous complex of boron ($B(OH_3)_{aq}$). Similar fractionation patterns were also observed for the neutral $HCl_{(aq)}$ aqueous species as it is referred from the linear-steady decrease of pH at low water-density conditions (inset plot).

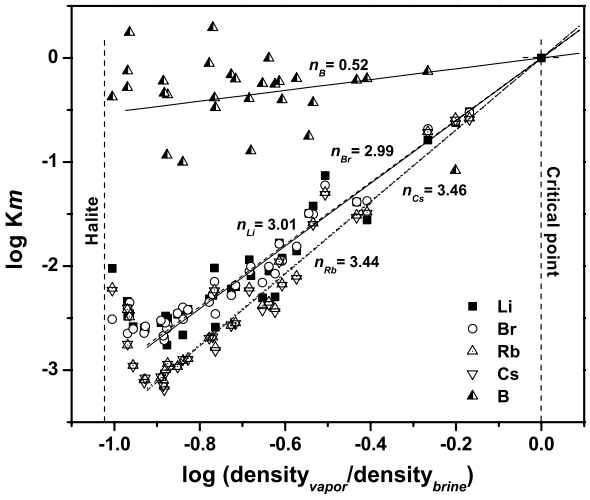

Fig. 5. Ray diagram constructed to evaluate apparent partitioning coefficients (K_m) as function of density ratios between vapors and brines. The slope of the lines expressed as (n_i) describes the relative tendency of elements to partition into vapor phase. The overall extent of enrichment into vapors decreases in the order B > Li ≅ Br > Rb ≅ Cs, with B showing a strong volatile behavior attributed to the presence of gaseous hydroxide aqueous species. The reversal in partitioning direction (negative slope) observed for Li, Br, Rb and Cs is likely caused by the increasingly ionic character of brine near the halite stability field, which enhances *salting-out* effects.

gas-like $B(OH)_{3(aq)}$ species at elevated temperatures and pressures.

Strong volatile tendencies not only characterize dissolved gases (e.g. $H_{2(aq)}$, $H_2S_{(aq)}$, $CO_{2(aq)}$ (Smith et al., 1987)) and some hydroxide aqueous species, but also many other neutral aqueous complexes, especially in hydrothermal systems at extreme conditions of temperature and pressure. For example, despite the apparent non-volatile trend in the ray diagram (Fig. 5) for Li, Br, Rb and Cs (n_i = positive), when pressure–temperature conditions approach the halite stability field, an abrupt change in hydration/solvation occurs that gives rise to negative correlation between $\log(K_m)$ and density when $\log(\text{density}_{vapor}/\text{density}_{brine})$ is less than ~−0.9 (Fig. 5). These conditions reflect brine compositions (wt% NaCl) ranging from approximately 40% (250 bars) to 60% (350 bars), and suggest that the increasing brine composition becomes unusually effective in excluding (*salting-out*) neutral aqueous complexes, as inferred earlier. In fact, negative hydration and *salting-out* are closely related, as solvent molecules tend to hydrate electrolyte ions rather than non-electrolyte molecules (Grover and Ryall, 2004). Thus, under unusually low-density conditions, typically non-volatile aqueous species can achieve some measure of volatility.

The ray diagram, however, can be only constructed for the two fluid phases (vapor–brine) and does not permit assessment of trace element partitioning involving halite-fluid equilibria. Therefore, a different approach, one that emphasizes chloride-normalized trends is used to provide data for partition coefficients of Li, Br, Rb, and Cs between halite and coexisting vapor and/or brine.

4.2. Cl-normalized partitioning coefficients

An important advantage of using element/Cl ratios to assess trace element partitioning in multiphase systems is the minimal effects of bulk fluid composition on the apparent

partitioning coefficients (K_m) of elements that exist largely if not entirely complexed with chloride (e.g. Li, Cs, Rb), or sodium (in the case of Br), which is linked to Cl through electrical neutrality constraints (Shock et al., 1997; Sverjensky et al., 1997).

The similar fractionation models observed for the Li–Br and Cs–Rb pairs determined from constraints imposed by hydration–solvation effects (n_i) agree well with somewhat analogous data derived from correlations between chloride-normalized trace element concentrations ($D_{el/Cl}$) and the density of water (ρ_w). In detail, the virtually identical trends for Li–Br and Rb–Cs obtained by the latter method (Fig. 6) are consistent with predictions based on differences in the electronegativity of the elements constituting the dominant form of the dissolved species (Berndt and Seyfried, 1990). Thus, it appears that Br and Li have a significant tendency to partition into vapors (Fig. 6a), while Rb and Cs favor fractionation into the high-salinity fluids (Fig. 6b). These data are in good agreement with partitioning coefficients derived from previous phase separation experiments (Berndt and Seyfried, 1990, 1997), although these earlier studies were largely restricted to pressure and temperature conditions close to the two-phase boundary. Despite the inverse partitioning behavior of Li–Br and Rb–Cs for vapor–brine equilibria, upon intersection of the halite–vapor ± brine field (Fig. 1), both trace element pairs reveal a dramatic enhancement in partitioning into the vapor (low salinity) phase, most likely encouraged by trace element exclusion from the halite structure (Tosi and Doyama, 1966). Apparently, not only Br is excluded from NaCl mineral phases (Oosting and Von Damm, 1996; Berndt and Seyfried, 1997), but also other elements that are largely transported as aqueous chloro-complexes. This could have important implications for reconstructing conditions of hydrothermal alterations from the relative abundances of trace alkali elements in vapors and fluid inclusions from modern and ancient hydrothermal systems that reveal evidence of extreme phase separation and halite precipitation/dissolution processes.

The apparent correlation between $D_{el/Cl}$ and water density (ρ_w) (Fig. 6) permits $D_{el/Cl}$ values to be expressed as function of ρ_w as follows:

$$\log(D_{el/Cl}) = a + b\log(\rho_w) + c\log(\rho_w)^2 + d\log(\rho_w)^3 \qquad (7)$$

where a, b, c, d are coefficients unique to specific trace elements (Table 2). The expression is valid for a density range from 0.094 to 0.28 g/cm^3, that includes pressure and temperature conditions of the present study.

Trace element partitioning involving vapor–brine and halite–vapor equilibria is largely indistinguishable between subcritical and supercritical conditions. Indeed, experimental data indicate the over-riding importance of water density, and crystal chemical effects imposed by halite on the direction and magnitude of trace element partitioning in the multiphase NaCl–H_2O system. Thus, classifying phase separation as subcritical or supercritical based on pressure and temperature conditions relative to the critical point of

Table 2
Fit and correlation coefficients that describe element partitioning in the two-phase NaCl–H_2O system (Eq. (7))

	Br	Li	Rb	Cs
a	−13.04	−10.29	−23.43	−23.94
b	−54.95	−44.36	−102.95	−105.20
c	−76.93	−64.05	−148.98	−152.28
d	−36.09	−31.14	−70.71	−72.31
r^2	0.92	0.87	0.90	0.90
Root-MSE	0.11	0.17	0.19	0.20

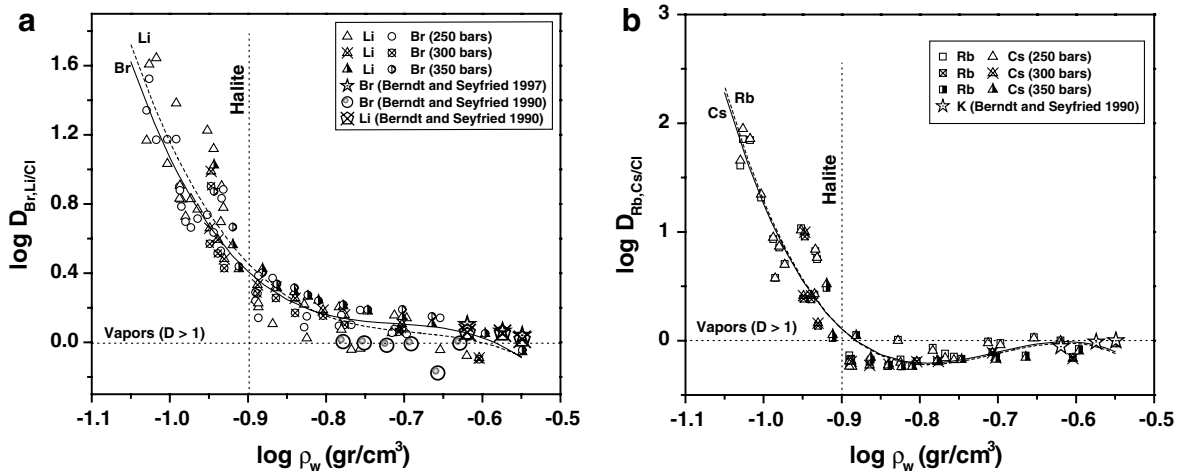

Fig. 6. Distribution of Cl-normalized partitioning coefficients ($D_{el,Cl}$) between vapor–brines and halite–vapor in terms of water density. Results clearly demonstrate the tendency of Br and Li to partition into vapors (a), while Rb and Cs are more enriched in brines (b). This overall trend is consistent with results from previous phase separation experiments that were largely confined to pressure and temperature conditions close to the critical curve. Interestingly, potassium partitioning coefficients are in close agreement with $D_{Rb,Cs/Cl}$ values (b), consistent with the effect predicted by the similar electronegativity differences in the dominant aqueous complexes of Rb, Cs and K on the vapor–brine fractionation trends. Upon intersection of the halite–vapor–brine boundary, however, Li–Br and Rb–Cs pairs partition greatly into the vapor, supporting a strong trace element exclusion from the mineral structure.

seawater (407 °C—298 bars) (Bischoff and Rosenbauer, 1985), is in and of itself, not particularly meaningful as a guide to trace element systematics in subseafloor hydrothermal fluids. Accordingly, we advocate reference only to supercritical conditions in the NaCl–H_2O system, when these apply in subseafloor hydrothermal reaction zones.

4.3. Boron

Partition coefficients (K_m) data describing transfer of boron between vapor and coexisting brine (Fig. 5) support a volatile-like behavior of boron owing the enhanced stability of $B(OH)_{3(aq)}$ in low pH and low-density aqueous fluids (Schmidt et al., 2005), although previous experimental studies indicate otherwise for some conditions (Berndt and Seyfried, 1990; Liebscher et al., 2005). The extensive range of chemical and physical conditions examined during the present study, however, confirm fractionation of boron into vapor, especially for phase separation conditions far removed from the two-phase boundary of the NaCl–H_2O system. Under these conditions, the unusually high dissolved chloride of the brine acts to effectively exclude boron from the brine, as emphasized earlier. By expressing the ratio of dissolved boron in the vapor to that of the fluid prior to phase

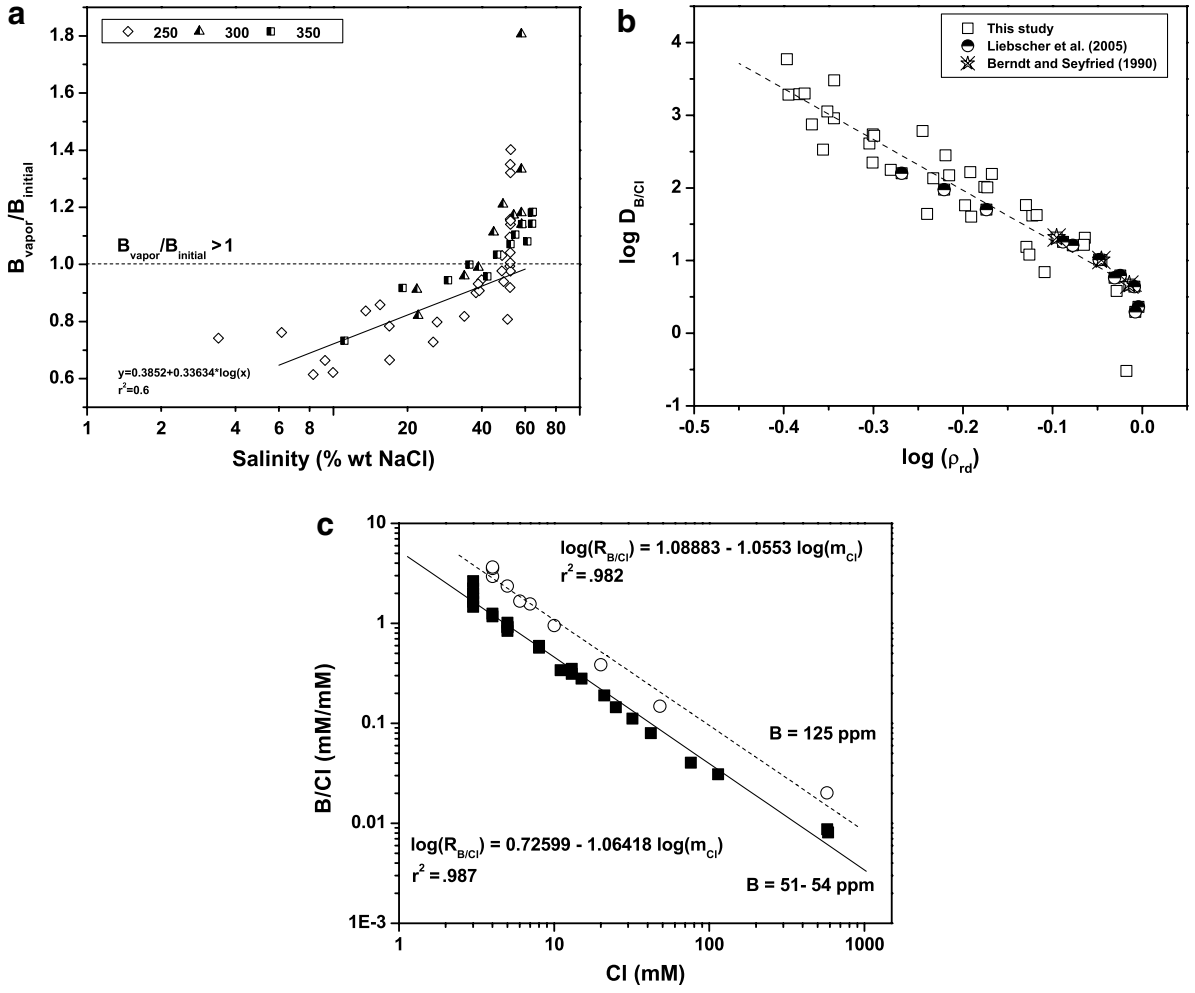

Fig. 7. Boron vapor–brine partitioning during phase separation experiments in the NaCl–H_2O system at elevated temperatures and pressures. Vapor enrichment observed for boron is most likely linked to *salting-out* phenomena of neutral dissolved molecules coexisting with highly ionic brines. (a) The effect of brine salinity on the ratio of dissolved B in vapors relative to the homogeneous starting solution suggests preference of B for the vapor at dissolved chloride concentrations of the coexisting brines in excess of ~40–50 wt% NaCl. Accordingly, B indicates immiscible behavior in saline fluids and NaCl mineral phases, resulting to higher than unity $B_{vapor}/B_{initial}$ ratios. In the case of lower brine salinities, however, B partitions weakly into the brine fraction being in close agreement with previous experimental studies. (b) A better understanding of B fractionation can be inferred if Cl-normalized partitioning coefficients ($D_{B/Cl}$) are expressed in terms of reduced density ($\rho_{rd} = \rho/\rho_{cr}$). Boron enrichment into vapors is indeed strongly correlated with the extent of phase separation as described by the deviation of H_2O density at conditions from density values along the critical curve. Results of previous experimental studies are in excellent agreement with those of the present study (regression analysis conducted by excluding the outlier data point near critical conditions). (c) Distribution of B/Cl ratios in supercritical vapors for homogeneous starting fluids with different B composition observed during the present experiments. Data suggest an overall conservative behavior of B during vapor–brine equilibria, as reflected by similar slopes of the fitting functions. Departures from the 1:1 relationship in natural hydrothermal systems suggest the possibility of boron addition by magmatic degassing processes.

separation, vapor enrichment of boron becomes even more clear, especially when the salinity of the coexisting brine exceeds ~40–50 wt% NaCl, at which point halite stability is achieved (Fig. 7a). At lower bulk chloride composition, boron does indeed appear to partition weakly into the brine, in general agreement with previous investigations (Berndt and Seyfried, 1990; Liebscher et al., 2005). Apparently, B is strongly immiscible in high-salinity fluid and mineral phases, allowing $B_{vapor}/B_{initial}$ ratios to reach values higher than unity. The incompatibility of B in fluids with highly elevated salt content, however, has also been suggested from fluid (vapor/brine)-saturated melt experiments (Schatz et al., 2004), where B partition coefficients indicative of vapor enrichment relative to brine ranged from 2 to 8. Thus, it is the salinity of the brine phases that governs the extent of vapor–brine B fractionation, a conclusion consistent with *salting-out* phenomena typical of neutral dissolved molecules in highly concentrated NaCl aqueous solutions (Pitzer and Schreiber, 1987; Oelkers and Helgeson, 1990; Oelkers and Helgeson, 1993a,b; Sharygin et al., 2002; Grover and Ryall, 2004). Accordingly, dilute vapor produced during extreme phase separation conditions in the NaCl–H_2O system could be expected to contain relatively high concentrations of dissolved boron on both an absolute and chloride-normalized basis. These data have important implications for the quantitative interpretation of mass transport processes involving boron at the magmatic–hydrothermal interface in subaerial and submarine settings.

An alternative approach to assess the magnitude of boron partitioning between vapor and brine is provided by correlating Cl-normalized distribution coefficients ($D_{B/Cl}$) with reduced density (ρ_{rd}), as follows[2]:

$$\log(D_{B/Cl}) = 0.570335 - 6.98584\log(\rho_{rd})^2 \quad (8)$$

where reduced density is defined as the ratio of the density of H_2O at experimental conditions with that along the critical curve (ρ/ρ_{cr}). A similar approach involving the departure of the actual pressure conditions from the critical curve has been successfully adopted to study hydrogen and boron isotopic systematics under two-phase conditions (Berndt et al., 1996; Liebscher et al., 2005). This approach for boron, however, reveals an excellent linear correlation over the full range of conditions investigated during the present and previous studies, which, as noted, tended to emphasize more narrow compositional conditions (Fig. 7b).

The conservative behavior of boron during phase separation reflected in the $D_{B/Cl}$–ρ_{rd} relationship, can be realized on even a more basic level by simply plotting the chloride-normalized boron concentration against dissolved Cl concentrations (Fig. 7c). The apparent identical linear correlation between B/Cl ratios and Cl retrieved for a range of pressure and temperature conditions (Fig. 4b), however, appears to be dependent on fluid compositional constraints induced prior to phase separation. Experiments (1, 2 and 3 at 250 bars) with two different initial B concentrations (50/125 ppm) illustrate this best, further supporting the firm conservative behavior of boron (Fig. 7c). The slopes of the linear functions, however, are almost identical, in compliance with the overall invariable enrichment of B into the vapor phases. Thus, phase separation processes seem to establish a linear relationship between B/Cl and Cl best described with a slope of 1:1.

This observation might have important implications in distinguishing major magmatic degassing from extreme phase separation events based on the distribution of B in low-salinity vent fluids. Boron derived from leaching of basalt followed by phase separation would almost certainly follow the described linear correlation, although addition of excess boron to the hydrothermal system from magmatic degassing would result in a more complex pattern likely defined by a steepening of the line segment for fluids having greatly dilute vapors. Indeed, the lack of a common line between B/Cl ratio and total dissolved Cl for a hydrothermal vent fluid system may be used to infer just such a process. To have these magmatic inputs overprinted on the Cl-normalized B distribution of vapor-rich vent fluids, however, requires magmatic contributions to be higher than 50% of the basalt-derived B fraction, which might not be the case for lower magnitude magmatic degassing events as those recognized in the high-temperature vapors sampled at Main Endeavour Field, northern Juan de Fuca Ridge (Foustoukos et al., 2004).

4.4. Supercritical phase separation in Brandon hydrothermal system (21°S EPR)

The Brandon hydrothermal field on the southern East Pacific Rise (21°S EPR) reveals vigorous venting with measured fluid temperatures reaching 405 °C (Von Damm et al., 2003). Most importantly, these high-T vent fluids appear to be conjugate vapor and brines pairs having dissolved Cl concentrations that deviate moderately from seawater, with phase separation suggested to occur very near the seafloor (287 bars), perhaps within the sulfide chimney structures (Von Damm et al., 2003). Despite the apparent reasonableness of such an interpretation, alternative scenarios are possible, especially if the bulk composition of the fluid is affected by phase *segregation* processes during subseafloor circulation (Seyfried et al., 2003). Application of constraints imposed by quartz solubility together with phase relations involving dissolved boron and Br, however, permit the development of an alternative model for subseafloor heat and mass transfer processes at the Brandon hydrothermal system.

Dissolved silica concentrations can be used to constrain subseafloor depth and temperature of water/rock interaction, assuming quartz-fluid equilibria. Experimental and theoretical data have helped to resolve the primary factors governing quartz solubility in chloride-bearing aqueous fluids, including temperature (°C), density of H_2O (ρ_w) (g/cm^3), and the molality of dissolved chloride (m_{cl}). Recently, these parameters have been incorporated into an algorithm optimized for the two-phase region in the NaCl–H_2O-system (Foustoukos and Seyfried, 2007).

$$\log m_{SiO_2(aq)} = -5.10347 + 0.00883565 * T_c + 0.105367\log m_{Cl} + 1.03419\log \rho_w \quad (9)$$

[2] Correlation coefficient $r^2 = 0.83$.

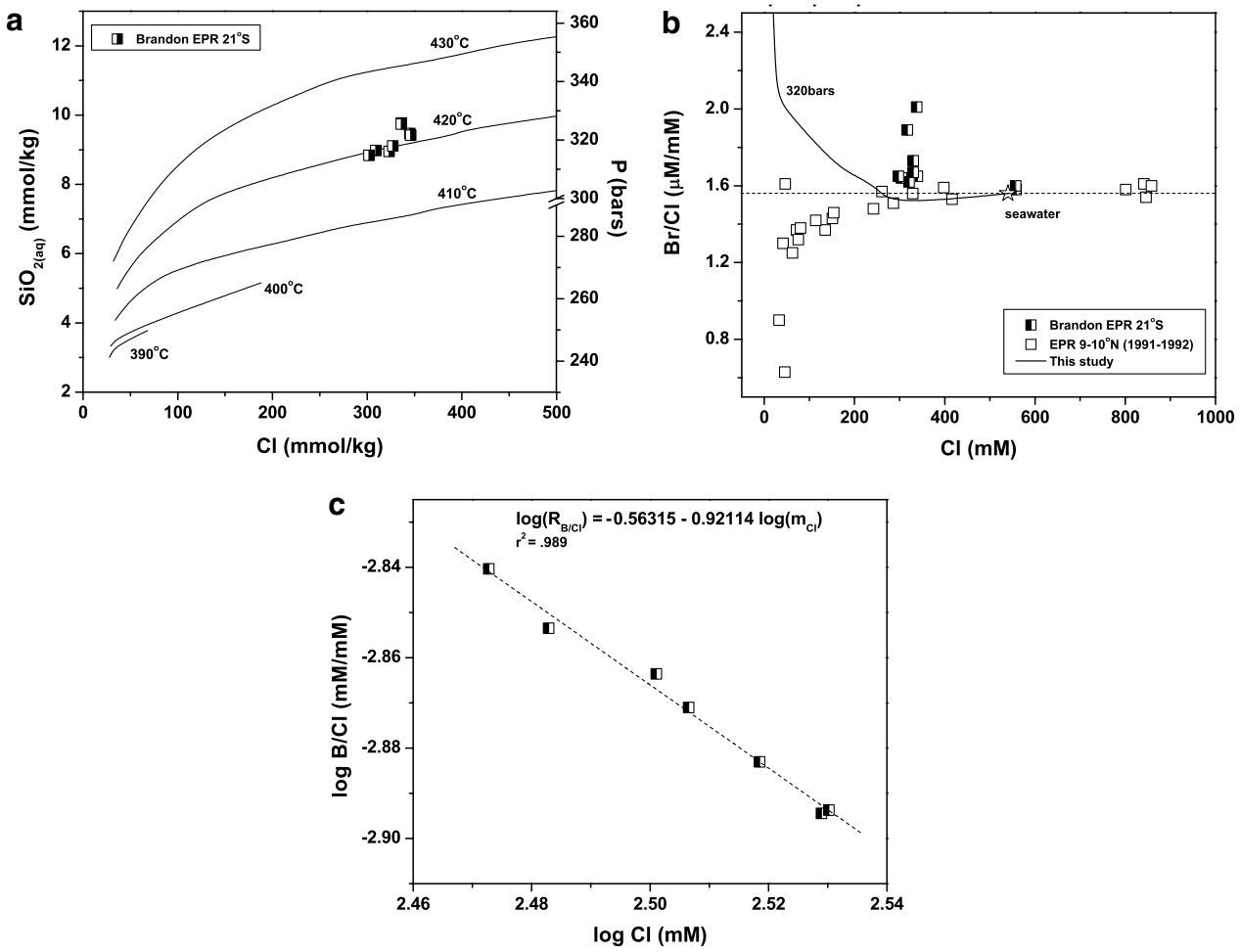

Fig. 8. Combination of phase equilibria approaches to constrain physical and chemical conditions in the subseafloor reaction zone of the Brandon hydrothermal system at 21°S EPR. (a) Application of quartz-fluid equilibria optimized for the two-phase NaCl–H_2O system (Foustoukos and Seyfried, 2007) indicates temperatures of approximately 420 °C and subseafloor depth of nearly 300 m below seafloor. (b) The significant deviation in Br/Cl ratios from seawater values is also observed for the Brandon vent fluids. High Br/Cl ratios can result during phase separation upon intersection of the halite stability where *salting-out* and crystal (halite) chemical effects greatly enhance Br enrichment in the coexisting vapor. Mixing of these vapor-rich (high Br/Cl) fluids with evolved-seawater at approximately 420 °C could account for the observed data. (c) The proposed near-seafloor magma source that fuels supercritical phase separation, however, is not contributing to B fluxes through magmatic degassing. Supporting evidence is the linear 1:1 correlation between B/Cl and total dissolved Cl for the Brandon vent fluids, which strongly suggests that rock–fluid interaction followed by supercritical phase separation accounts best for the Brandon data with little or no input of boron from another source.

In effect, the relatively high dissolved SiO_2 and chloride concentrations for the vapor-rich vent fluids at Brandon suggest subseafloor temperatures and pressures of approximately 420 °C and 320 bars, respectively (Fig. 8a). Thus, phase separation and water/rock interaction indicate *supercritical* conditions, some 300 m below seafloor. Although the proposed placement of the hydrothermal reaction zone at Brandon is relatively shallow, the depth is still sufficient for brine segregation to occur (Fontaine and Wilcock, 2006), with corresponding effects on the chemical and physical properties of the evolved hydrothermal fluid.

The chloride-normalized Br concentrations of the low-salinity fluids at Brandon (Table 3), however, show a clear increase relative to seawater (Fig. 8b), suggesting supercritical phase separation at conditions even more extreme than indicated by quartz-fluid equilibria (420 °C—320 bars). The Br/Cl enrichment is indeed significant, being comparable in magnitude with the change relative to seawater to that first observed in vent fluids from 9 to 10°N EPR, where halite dissolution was proposed (Oosting and Von Damm, 1996). The present experimental data indicate that vapor–brine partitioning (derived from Eq. (7)[3]) cannot account for the observed enrichment in Br/Cl, lending support for a model involving halite precipitation. If this is the case, then temperatures in excess of 450 °C are required, assuming a seawater source fluid and pressure of 320 bars (Fig. 1),

[3] The range of estimated $D_{Br/Cl}$ (0.9–1.6) allowed Br/Cl_{brine} to be considered equal to starting fluid values (seawater) (see Figs. 4a and 6a).

Table 3
Selected element concentrations from the Brandon vapor-rich vent fluids at 21°S EPR (Von Damm et al., 2003)

Orifice	T (°C)	Cl (mM[a])	$SiO_{2(aq)}$ (mM)	Br (μM)	B (μM)
Ba.1	404	317	8.78	600	434
Ba.2	405	338	9.28	680	431
Ba.3	401	339	9.23	560	433
Ba.5	400	330	9.58	570	
Bc.4	403	304	8.82	500	426
Bc.5		321	8.94	520	432
Bd.4	401	297	8.69	490	429
Bd.5	405	330	9.55	550	432

[a] mM, $mol/kg_{solution}$.

while the coexisting vapor would have Cl concentrations less than 10 $mmol/kg_{sol}$ (Fig. 3). Thus, the elevated Br/Cl ratios (>2) while indicating possible halite precipitation, are inconsistent with the observed P–T conditions of the vapor-rich vent fluids at Brandon and also with conditions imposed by quartz solubility constraints (420 °C, 320 bars).

One interpretation that can account for these apparently disparate observations involves mixing of a 420 °C evolved-seawater with a strongly Cl-depleted and Br/Cl-enriched supercritical vapor initially formed at temperatures sufficiently high to cause halite precipitation. Owing to the exponential increase in Br/Cl with decrease in dissolved chloride of the vapor-rich fluid coexisting with halite, even modest amounts of this fluid could greatly affect the Br/Cl ratio of the mixture. Accordingly, dissolved silica concentrations of the mixture may not be substantially altered. Even if dissolved silica were affected, re-equilibration of quartz (420 °C, 320 bars) could be quickly reestablished at these conditions (Dove and Crerar, 1990; Dove, 1999), although the same is not the case for the Br/Cl ratio, which provides strong and compelling evidence of a very high temperature component to the fluids venting at Brandon.

Despite the likelihood of a near-seafloor magma body sufficient to achieve supercritical conditions in the subseafloor reaction zone at Brandon, boron systematics preclude a significant input of magmatic-derived boron. Indeed, the slope of the line depicting B/Cl against dissolved Cl concentrations is virtually identical to that determined for boron partitioning between vapor and brine under supercritical conditions during the present investigation (Figs. 7c and 8c), providing strong evidence for similar processes occurring at Brandon. Thus, the boron data from Brandon (Table 3) are best interpreted as due to quantitative release of boron from basalt during hydrothermal alteration followed by preferential fractionation of the boron into the vapor phase. Accordingly, the boron data together with Br/Cl systematics and constraints imposed by quartz-fluid equilibria, strongly suggest hydrothermal alteration processes at Brandon dominated by *supercritical* phase separation. Such detailed analysis based on minor variations in trace element distributions, however, is only possible for the vapor-rich fluids at Brandon field, since the associated higher salinity fluids indicate both seawater entrainment (10% mixing) and conductive cooling (Von Damm et al., 2003), which obfuscate primary phase relations.

5. CONCLUSIONS

Experiments involving trace element partitioning between vapor–brine and halite–vapor in the NaCl–H_2O system were conducted to constrain the causes and implications of trace element/chloride variability now well recognized in subseafloor hydrothermal systems. In general, results indicate the preference of Li and Br to become enriched in low-chloride vapors, while Rb and Cs favor the brine throughout the range of chemical and physical conditions for which the two-phases coexist. This is best illustrated by the distribution of apparent (K_m) and Cl-normalized ($D_{el/Cl}$) partition coefficients across the P–T space of the vapor–brine phase region. Thus, data show a decrease in vapor enrichment in the order of $Li \cong Br > Rb \cong Cs$, which relates well to predictions based on electronegativity differences between the charged species constituting the dominant aqueous complex for each trace element. Partitioning changes abruptly, however, as the halite field of stability is approached, and is characterized by highly non-linear increases in trace element enrichment in the vapor for all species. The increasing dissolved chloride concentration of the brine enhances *salting-out* effects that drive neutral trace alkali halide and bromide complexes into the vapor. Vapor enrichment is enhanced further with halite formation owing to the incompatibility of the trace elements in halite lattice.

Compositional variability of dissolved boron during vapor–brine equilibria primarily relates to the polar and gas-like nature of the dominant B-bearing hydroxide aqueous species ($B(OH)_{3(aq)}$). These neutral aqueous species have a high volatility index and thus are highly sensitive to *salting-out* effects giving rise to strong enrichment in the vapor under all conditions investigated. Moreover, the experimental data reveal a robust linear correlation between Cl-normalized boron concentrations in vapors and the reduced density conditions (ρ/ρ_{cr}), which allow more accurate comparisons to be made with experimental data from other sources, while helping to constrain the geochemical implications of boron in vapors form natural hydrothermal systems. Furthermore, the conservative nature of boron during vapor–brine equilibria is confirmed by the 1:1 linear correlation between vapor B/Cl ratios and dissolved Cl concentrations.

Experimental calibration of the role of phase separation on trace element distributions provides a powerful tool that can be used with other phase equilibria data to better determine conditions of hydrothermal alteration in subseafloor reaction zones at mid-ocean ridges. For example, by coupling the experimentally determined B/Cl and Br/Cl partition data with constraints imposed by quartz solubility in the two-phase NaCl–H_2O system, we show that the vapor-dominated vent fluids issuing from the Brandon hydrothermal system (EPR 21°S) are most likely derived by *supercritical* phase separation fueled by a shallow magmatic body; showing no indication of major magmatic degassing but strongly supporting subsurface mixing with highly Cl-depleted and Br-enriched vapor fluids produced under halite precipitation conditions.

ACKNOWLEDGMENTS

This work was made possible after financial support provided through NSF Grants OCE-0221031 and OCE-0351069. Special thanks to Rick Knurr (Department of Geology and Geophysics at the University of Minnesota) for development of new analytical approaches without which the study could not have been conducted. We would also like to thank Dr. Mike Berndt for his important contribution in the design of the flow-through system.

REFERENCES

Anderko A., and Pitzer K. S. (1993) Equation of state representation of phase equilibria and volumetric properties of NaCl–H_2O above 573 °C. *Geochim. Cosmochim. Acta* **57**, 1657–1680.

Audetat A., Gunther D., and Heinrich C. A. (1998) Formation of a magmatic–hydrothermal ore deposit: insights with LA-ICP-MS analysis of fluid inclusions. *Science* **279**, 2091–2093.

Berndt, M. E., Person, M. E., and Seyfried Jr., W. E. (2001) Phase separation and two-phase flow in seafloor hydrothermal systems: Geophysical modeling in the NaCl–H_2O system. In *Eleventh Annual V. M. Goldschmidt Conference*. Geochemical Society, Hot Springs, Va.

Berndt M. E., Seal, II, R. R., Shanks, III, W. C., and Seyfried, Jr., W. E. (1996) Hydrogen isotope systematics of phase separation in submarine hydrothermal systems: experimental calibration and theoretical models. *Geochim. Cosmochim. Acta* **60**, 1595–1604.

Berndt M. E., and Seyfried, Jr., W. E. (1990) Boron, bromine, and other trace elements as clues to the fate of chlorine in mid-ocean ridge vent fluids. *Geochim. Cosmochim. Acta* **54**, 2235–2245.

Berndt M. E., and Seyfried, Jr., W. E. (1997) Calibration of Br/Cl fractionation during subcritical phase separation of seawater; possible halite at 9 to 10°N East Pacific Rise. *Geochim. Cosmochim. Acta* **61**, 2849–2854.

Bischoff J. L. (1991) Densities of liquids and vapors in boiling NaCl–H_2O solutions; a PVTx summary from 300° to 500 °C. *Am. J. Sci.* **291**, 309–338.

Bischoff J. L., and Rosenbauer R. J. (1984) The critical point and two-phase boundary of seawater, 200–500 °C. *Earth Planet. Sci. Lett.* **68**, 172–180.

Bischoff J. L., and Rosenbauer R. J. (1985) An empirical equation of state for hydrothermal seawater (3.2% NaCl). *Am. J. Sci.* **285**, 725–763.

Bischoff J. L., and Rosenbauer R. J. (1987) Phase separation in seafloor geothermal systems: an experimental study on the effects of metal transport. *Am. J. Sci.* **287**, 953–978.

Bischoff J. L., and Rosenbauer R. J. (1988) Liquid–vapor relations in the critical region of the system sodium chloride–water from 380 to 415 °C: a refined determination of the critical point and two-phase boundary of seawater. *Geochim. Cosmochim. Acta* **52**, 2121–2126.

Bischoff J. L., Rosenbauer R. J., and Fournier R. O. (1996) The generation of HCl in the system $CaCl_2$–H_2O: vapor–liquid relations from 380–500 °C. *Geochim. Cosmochim. Acta* **60**, 7–16.

Butterfield, D. A., Jonasson, I. R., Massoth, G. J., Feely, R. A., Roe, K. K., Embley, R. E., Holden, J. F., McDuff, R. E., Lilley, M. D., and Delaney, J. R. (1999) Seafloor eruptions and evolution of hydrothermal fluid chemistry. In *Mid-Ocean Ridges; Dynamics of Processes Associated with Creation of New Ocean Crust* (eds. J. R. Cann, H. Elderfield, and A. Laughton).

Butterfield D. A., McDuff R. E., Mottl M. J., Lilley M. D., Lupton J. E., and Massoth G. J. (1994) Gradients in the composition of hydrothermal fluids from the Endeavor segment vent field: phase separation and brine loss. *J. Geophys. Res.* **99**, 9561–9583.

Chan L. H., Edmond J. M., and Thompson G. (1993) A lithium study of hot springs and metabasalts from mid-ocean ridge hydrothermal systems. *J. Geophys. Res.* **98**, 9653–9659.

Cook D. R., and Weisberg S. (1999) *Applied Regression Including Computing and Graphics*. Wiley-Interscience.

Davies C. W. (1962) *Ion Association*. Butterworths, London, London.

Dove P. M. (1999) The dissolution kinetics of quartz in aqueous mixed cation solutions. *Geochim. Cosmochim. Acta* **63**, 3715–3727.

Dove P. M., and Crerar D. A. (1990) Kinetics of quartz dissolution in electrolyte solutions using a hydrothermal mixed flow reactor. *Geochim. Cosmochim. Acta* **54**, 955–969.

Driesner T., Seward T. J., and Tironi I. G. (1998) Molecular dynamics simulation study of ionic hydration and ion association in dilute and 1 molal aqueous solutions from ambient to supercritical conditions. *Geochim. Cosmochim. Acta* **62**, 3095–3107.

Fontaine F. J., and Wilcock W. S. (2006) Dynamics and storage of brine in mid-ocean ridge hydrothermal systems. *J. Geophys. Res.* **111**. doi:10.1029/2005JB003866.

Fornari D. J., Shank T., Von Damm K. L., Gregg T. K. P., Lilley G., Levai G., Bray A., Haymon R. M., Perfit M. R., and Lutz (1998) Time-series temperature measurements at high-temperature hydrothermal vents, East Pacific Rise 9°49'–51'N: evidence for monitoring a crustal cracking event. *Earth Planet. Sci. Lett.* **160**, 419–431.

Fournier, R.O. (1986) Conceptual models for brine evolution in magmatic–hydrothermal systems. In: *U.S. Geological Survey* (eds. R. W. Decker, T. L. Wright, and P. H. Stauffer).

Foustoukos D. I., James R. H., Berndt M. E., and Seyfried, Jr., W. (2004) Lithium isotopic systematics of hydrothermal vent fluids at the Main Endeavour Field, Northern Juan de Fuca Ridge. *Chem. Geol.* **212**, 17–26.

Foustoukos D. I., and Seyfried W. E. J. (2007) Quartz solubility in the two-phase and critical region of the NaCl–KCl–H_2O system: implications for submarine hydrothermal vent systems at 9°50'N East Pacific Rise. *Geochim. Cosmochim. Acta* **71**, 186–201.

Fulton J. L., Pfund D. M., Wallen S. L., Newville M., Stern E. A., and Ma Y. (1996) Rubidium ion hydration in ambient and supercritical water. *J. Chem. Phys.* **105**, 2161–2166.

Grover P. K., and Ryall R. L. (2004) Critical appraisal of salting-out and it's implications for chemical and biological sciences. *Chem. Rev.* **105**, 10.1021/cr030454p.

Haar L., Gallagher J. S., and Kell G. S. (1984) *NBS/NRC Steam Tables: Thermodynamic and Transport Properties and Computer Programs for Vapor and Liquid States of Water in SI Units*.

Haas J. L. (1976a) Physical properties of the coexisting phases and thermochemical properties of the H_2O component in boiling NaCl solutions, preliminary steam tables for NaCl solutions. *Geol. Surv. Bull.* **1421-A**, 73 p. (report).

Haas J. L. (1976b) Thermodynamic properties of the coexisting phases and thermochemical properties of the NaCl component in boiling NaCl solutions. *Geol. Surv. Bull.* **1421-B**, 71 p. (report).

Hayba D. O. and Ingebritsen S. E. (1994) The computer model Hydrotherm, a three-dimensional finite-difference model to simulate ground-water flow and heat transport in the temperature range of 0 to 1,200 °C. *U.S. Geological Survey, Open-File Report*.

Heinrich C. A., Driesner T., Stefansson A., and Seward T. J. (2004) Magmatic vapor contraction and the transport of gold from the

porphyry environment to epithermal ore deposits. *Geology* **32**, 761–764.

Ho P. C., Bianchi H., Palmer D. A., and Wood R. H. (2000a) Conductivity of dilute aqueous electrolyte solutions at high temperatures and pressures using a flow cell. *J. Solut. Chem.* **29**, 217–235.

Ho P. C., Palmer D. A., and Gruszkiewicz M. S. (2001) Conductivity measurements of dilute aqueous HCl solutions to high temperatures and pressures using a flow-through cell. *J. Phys. Chem. B* **105**, 1260–1266.

Ho P. C., Palmer D. A., and Mesmer R. E. (1994) Electrical conductivity measurements of aqueous sodium chloride solutions to 600 °C and 300 MPa. *J. Solut. Chem.* **23**, 997–1018.

Ho P. C., Palmer D. A., and Wood R. H. (2000b) Conductivity measurements of dilute aqueous LiOH, NaOH, and KOH solutions to high temperatures and pressures using a flow-through cell. *J. Phys. Chem. B* **104**, 12084–12089.

Liebscher A., Meixner A., Romer R. L., and Heinrich W. (2005) Liquid–vapor fractionation of boron and boron isotopes: experimental calibration at 400 °C/23 MPa to 450 °C/42 MPa. *Geochim. Cosmochim. Acta* **69**, 5693–5704.

Lilley M. D., Butterfield D. A., Lupton J. E., and Olson E. J. (2003) Magmatic events can produce rapid changes in hydrothermal vent chemistry. *Nature* **422**, 878–881.

Mercer J. W., and Faust C. R. (1979) Review of numerical simulation of hydrothermal systems. *Hydrolog. Sci. Bull.* **24**, 335–344.

Oelkers E. H., and Helgeson H. C. (1990) Triple-ion anions and polynuclear complexing in supercritical electrolyte solutions. *Geochim. Cosmochim. Acta* **54**, 727–738.

Oelkers E. H., and Helgeson H. C. (1993a) Calculation of dissociation constants and the relative stabilities of polynuclear clusters of 1:1 electrolytes in hydrothermal solutions at supercritical pressures and temperatures. *Geochim. Cosmochim. Acta* **57**, 2673–2697.

Oelkers E. H., and Helgeson H. C. (1993b) Multiple ion association in supercritical aqueous solutions of single electrolytes. *Science* **261**, 888–891.

Oosting S. E., and Von Damm K. L. (1996) Bromide/chloride fractionation in seafloor hydrothermal fluids from 9–10°N East Pacific Rise. *Earth Planet. Sci. Lett.* **144**, 133–145.

Palmer, D. A., Simonson, J. M., and Jensen, J. P., 2004. Partitioning of electrolytes to steam and their solubilities in steam. In *Aqueous Systems at Elevated Temperatures and Pressures* (eds. D.A. Palmer, R. Fernandez-Prini and A.H. Harvey). Elsevier, New York, pp. 409–441.

Palmer M. R., and Edmond J. M. (1989) Cesium and rubidium in submarine hydrothermal fluids: evidence for recycling of alkali elements. *Earth Planet. Sci. Lett.* **95**, 8–14.

Pitzer K. S., Peiper J. C., and Busey R. H. (1984) Thermodynamic properties of aqueous sodium chloride solutions. *J. Phys. Chem. Ref. Data* **13**, 1–102.

Pitzer K. S., and Schreiber D. R. (1987) The restricted primitive model for ionic fluids: properties of the vapor and the critical region. *Mol. Phys.* **60**, 1067–1078.

Pokrovski G. S., Roux J., and Harrichourry J. C. (2005) Fluid density control on vapor–liquid partitioning of metals in hydrothermal systems. *Geology* **33**, 657–660.

Pokrovski G. S., Schott J., and Sergeyev A. S. (1995) Experimental determination of the stability constants of $NaSO_4^-$ and $NaB(OH)_4^o$ in hydrothermal solutions using a new high-temperature sodium selective glass electrode—Implications for boron isotopic fractionation. *Chem. Geol.* **124**, 253–265.

Pokrovski G. S., Zakirov I. V., Roux J., Testemale D., Hazemann J. L., Bychkov A. Y., and Golikova G. V. (2002) Experimental study of arsenic speciation in vapor phase to 500 °C: implications for As transport and fractionation in low-density fluids and volcanic gases. *Geochim. Cosmochim. Acta* **66**, 3453–3480.

Schatz O. J., Dolejs D., Stix J., Williams-Jones A. E., and Layne G. (2004) Partitioning of boron among melt, brine and vapor in the system haplogranite–H_2O–NaCl at 800 °C and 100 MPa. *Chem. Geol.* **210**, 135–147.

Schmidt C., Thomas R., and Heinrich W. (2005) Boron speciation in aqueous solutions at 22 to 600 °C and 0.1 MPa to 2 GPa. *Geochim. Cosmochim. Acta* **69**, 275–281.

Sengers J. M. H. L., Kamgar-Parsi B., Balfour F. W., and Sengers J. V. (1983) Thermodynamic properties of steam in the critical region. *J. Phys. Chem. Ref. Data* **12**, 1–28.

Seyfried, Jr., W. E., Chen X., and Chan L.-H. (1998) Trace element mobility and lithium isotope exchange during hydrothermal alteration of seafloor weathered basalt: An experimental study at 350 °C, 500 bars. *Geochim. Cosmochim. Acta* **62**, 949–960.

Seyfried, Jr., W. E., Seewald J. S., Berndt M. E., Ding K., and Foustoukos D. I. (2003) Chemistry of hydrothermal vent fluids from the Main Endeavour Field, Northern Juan de Fuca Ridge: Geochemical controls in the aftermath of June 1999 seismic events. *J. Geophys. Res.* **108**, 2429.

Seyfried, W. E. J., Janecky, D. R., and Berndt, M. E. (1987). Rocking autoclaves for hydrothermal experiments: II. The flexible reaction-cell system. In *Hydrothermal Experimental Techniques* (eds. H. Barnes and G. Ulmer). Wiley-Interscience, New York, pp. 216–239.

Sharygin A. V., Wood R. H., Zimmerman G. H., and Balashov V. (2002) Multiple ion association versus redissociation in aqueous NaCl and KCl at high temperatures. *J. Phys. Chem. B* **106**, 7121–7134.

Shock E. L., Sassani D. C., Willis M., and Sverjensky D. A. (1997) Inorganic species in geologic fluids: correlations among standard molal thermodynamic properties of aqueous ions and hydroxide complexes. *Geochim. Cosmochim. Acta* **61**, 907–950.

Simonson J. M., Palmer D. A., and Gruszkiewicz M. S. (2000) Liquid–vapor partitioning of aqueous electrolytes at temperatures to the solvent critical point. In *14th Symposium on Thermophysical Properties*, Boulder, Colorado, USA.

Smith C. L., Ficklin W. H., and Thompson J. M. (1987) Concentrations of arsenic, antimony, and boron in steam and steam condensate at the geysers, California. *J. Volcanol. Geoth. Res.* **32**, 329–341.

Spivack A. J., and Edmond J. M. (1987) Boron isotope exchange between seawater and the oceanic crust. *Geochim. Cosmochim. Acta* **51**, 1033–1043.

Stoessel R. K. (1992) Comment on "Reaction paths and equilibrium end-points in solid-solution systems" by P.J. Glynn, E.J. Reardon, L.N. Plummer and E. Busenberg. *Geochim. Cosmochim. Acta* **56**, 2555–2557.

Stoessel R. K., and Carpenter A. B. (1986) Stoichiometric saturation tests of $NaCl_{1-x}Br_x$, and $KCl_{1-x}Br_x$. *Geochim. Cosmochim. Acta* **50**, 1465–1474.

Styrikovich M. A. (1956) Investigation of steam contamination and the structure of the steam–water mixture by means of radioactive isotopes. In *Conf. Acad. Sci. U.S.S.R. on Peaceful Uses of Atomic Energy, Session Div. Tech. Sci.*, pp. 119–127.

Styrikovich M. A., Khaibullin I. K., and Tskhvirashvili D. G. (1955) Solubility of salts in high-pressure steam. *Dokl. Akad. Nauk SSSR* **100**, 1123–1126.

Styrikovich M. A., Tshvirashvili D. G., and Hebieridze D. P. (1960) A study of the solubility of boric acid in saturated water vapor. *Dokl. Akad. Nauk* **134**, 615–617.

Sue K., and Arai K. (2004) Specific behavior of acid-base and neutralization reactions in supercritical water. *J. Supercrit. Fluid* **28**, 57–68.

Sverjensky D. A., Shock E. L., and Helgeson H. C. (1997) Prediction of the thermodynamic properties of aqueous metal complexes to 1000 °C and 5 kb. *Geochim. Cosmochim. Acta* **61**, 1359–1412.

Tanger J. C. I. V., and Pitzer K. S. (1989) Thermodynamics of $NaCl–H_2O$: a new equation of state for the near critical region and comparisons with other equations for adjoining regions. *Geochim. Cosmochim. Acta* **53**, 973–987.

Tierney, L. (1989) *XLISP-STAT: A statistical environment based on the XLISP language (Version 2.0)*. School of Statistics, University of Minnesota, Minneapolis.

Tosi M. P., and Doyama M. (1966) Vacancies and monovalent cation impurities in the alkali halides. *Phys. Rev.* **151**, 642–648.

Von Damm K. L. (2000) Chemistry of hydrothermal vent fluids from 9°–10°N, East Pacific Rise; ''time zero,'' the immediate posteruptive period. *J. Geophys. Res.* **105**, 11203–11222.

Von Damm K. L., Buttermore L. G., Oosting S. E., Bray A. M., Fornari D. J., Lilley M. D., and Shanks, III, W. C. (1997) Direct observation of the evolution of a seafloor 'black smoker' from vapor to brine. *Earth Planet. Sci. Lett.* **149**, 101–111.

Von Damm K. L., Lilley M. D., Shanks W. C., Brockington M., Bray A. M., O'Grady K. M., Olson E., Graham A., and Proskurowski G. (2003) Extraordinary phase separation and segregation in vent fluids from the southern East Pacific Rise. *Earth Planet. Sci. Lett.* **206**, 365–378.

Von Damm K. L., Oosting S. E., Kozlowski R., Buttermore L. G., Colodner D. C., Edmonds H. N., Edmond J. M., and Grebmeier J. M. (1995) Evolution of East Pacific Rise hydrothermal vent fluids following a volcanic eruption. *Nature* **375**, 47–50.

Wallen S. L., Palmer B. J., Pfund D. M., Fulton J. L., Newville M., Ma Y., and Stern E. A. (1997) Hydration of bromide ion in supercritical water: an X-ray absorption fine structure and molecular dynamics study. *J. Phys. Chem. A* **101**, 9632–9640.

Associate editor: Jeffrey C. Alt